IET Systems Biology

WILEY

The Institution of Engineering and Technology

ORIGINAL RESEARCH OPEN ACCESS

Novel Biomarker Identification for Acute Coronary Syndrome via Integrating WGCNA and Machine Learning

Jie Zheng[1] | Fan Gong[2] | Liping Zhu[3] | Yin Zhang[4]

[1]Department of Cardiology, Tianyou Hospital Affiliated to Wuhan University of Science and Technology, Wuhan, China | [2]Cardiovascular Medicine Department, Wuhan Puren Hospital, Wuhan, China | [3]Department of Endocrinology, Huaihe Hospital of Henan University, Kaifeng, China | [4]Department of Cardiology, Rudong Hospital of TCM, Nantong, China

Correspondence: Yin Zhang (zhangyinrdtcm@163.com)

Received: 29 April 2025 | **Revised:** 14 July 2025 | **Accepted:** 31 July 2025

Handling Editor: Hao Wu

Funding: This work was funded by Nantong Scientific Research Project, Project Number MSZ2022098.

Keywords: bioinformatics | cardiovascular system | data mining | genomics

ABSTRACT

Immune cells in early atherosclerotic lesions promote inflammation and acute coronary syndrome (ACS), but the precise link between inflammation and ACS progression is still unclear. In this study, we analysed mRNA and miRNA expression profiles of ACS from GEO, identifying 98 mRNAs and 627 miRNAs by differentially expressed analysis. GSEA revealed abnormal activation of immune- and inflammation-related pathways, such as T cell receptor signalling pathway and cell adhesion molecules cams. The biomarkers ARG1, HECW2, and PFKFB3 were identified through WGCNA, LASSO, and SVM-RFE. Diagnostic performance and miRNA–mRNA interaction network were performed using ROC curves and Cytoscape. CIBERSORT analysis revealed that the levels of CD4 memory resting T cells were downregulated, whereas monocytes and neutrophils were upregulated. ARG1, HECW2 and PFKFB3 showed close relationships with specific immune cell types. These findings offer new avenues for ACS treatments and identify ARG1, HECW2 and PFKFB3 as potential biomarkers.

1 | Introduction

Acute coronary syndrome (ACS) is an acute manifestation of coronary heart disease, typically characterised by persistent chest pain and tightness [1]. It poses serious health risks, including arrhythmias, heart failure and even sudden cardiac death [2]. The primary cause of ACS is atherosclerosis, with key pathological and physiological processes including intimal damage, plaque rupture, vasospasm, platelet aggregation and thrombosis [3]. ACS can be broadly classified into two scenarios: (1) When an unstable atherosclerotic plaque ruptures, it can lead to the formation of an acute thrombus that causes vascular occlusion, resulting in acute ST-segment elevation myocardial infarction (STEMI). (2) If the occlusion is partial, it may lead to non-ST-segment elevation myocardial infarction (NSTEMI) or unstable angina [4, 5]. According to the Chinese Cardiovascular Health Report, by 2021, the mortality rates of coronary heart disease have exceeded 120 per 100000 and 130 per 100000 in urban and rural, respectively, with projections indicating a continued rise in the future [6]. Despite extensive research on ACS, there have been no breakthroughs that have translated into clinical treatment. Therefore, gaining a deeper understanding of the basic mechanisms is crucial for identifying potential clinical targets for ACS.

Immune cells play a critical role in the progression from atherosclerotic plaque rupture to platelet activation, acute thrombus formation, and subsequent vascular occlusion leading to acute

Jie Zheng and Fan Gong contributed equally to this work.

tissue damage [7]. Increasingly, studies are focusing on immune cells and inflammatory markers to improve risk stratification for ACS [8]. Several research studies have confirmed that multiple immune cells, including monocytes, macrophages and different lymphocyte subsets, are involved in chronic inflammatory responses that drive the progression of ACS [9, 10]. However, the precise relationship between immune cells and the development of unstable arterial plaques remains incompletely understood. MicroRNAs (miRNAs), typically about 22 nucleotides in length, impact gene expression by binding to promoter sequences and target regions [11]. Dysregulated miRNA expression is associated with various diseases, including ACS. miR-483-5p in serum of ACS, for example, has been identified as a promising biomarker, with studies showing that its levels are elevated in ACS patients and can forecast significant cardiovascular events after surgical treatment [12]. The level of miR-155 is notably reduced in individuals with coronary artery disease, and it plays a crucial role in modulating the release of inflammatory mediators in monocyte-derived dendritic cells and macrophages [13, 14].

Research studies indicate that the downregulation of miR-10a results in the triggering of the IκB/NF-κB, consequently increasing the levels of inflammatory markers in both experimental animal models and in vitro studies of atherosclerosis [15]. Indeed, it is demonstrated that miRNAs are integral in governing the developmental stages, maturation and ageing processes of diverse immune cells, impacting immune responses [16]. Innovations in sequencing technologies have enabled the identification of notable alterations in the miRNA profile associated with these processes [17, 18]. By targeting multiple targets, these miRNAs play a pivotal role in influencing the worsening and outcomes of atherosclerosis.

This study utilised GEO public data and bioinformatics assessment to contrast the differences in miRNA and mRNA profiles in peripheral blood samples between ACS patients and healthy controls. By establishing a preliminary miRNA–mRNA network related to ACS, the study also explored changes in immune cell infiltration associated with the condition. Additionally, the results suggest that ARG1, HECW2, and PFKFB3 could serve as promising biomarkers for ACS. Identifying novel biomarkers not only enhances our understanding of ACS pathogenesis but also facilitates earlier and more accurate diagnosis. ARG1, HECW2, and PFKFB3 could complement existing diagnostic methods (e.g., troponin assays) and inform individualised therapy by linking immune activation to clinical outcomes.

2 | Methods

2.1 | Data Retrieval and Download

Search for the keyword 'acute coronary syndrome' in the GEO (https://www.ncbi.nlm.nih.gov/geo/) database, filter for transcriptome sequencing or microarray data, and verify that the sample species, quantity and phenotype are clearly defined. The selected dataset should explicitly indicate that the samples correspond to acute coronary syndrome, with each group containing at least six samples. The ACS-related microarray datasets GSE60993, GSE61144 and GSE94605 were downloaded. These datasets were selected based on criteria, including clear phenotype annotation, sample size (≥ 6 per group), availability of both mRNA and miRNA profiles and a uniform sample source (peripheral blood). GSE60993 and GSE94605 offered complementary mRNA and miRNA data, whereas GSE61144 provided an independent cohort for validation.

All samples in these datasets are derived from human peripheral blood. GSE60993 consists of 7 healthy controls and 26 ACS patients, GSE61144 includes 10 healthy controls and 14 ACS patients, and GSE94605 comprises 7 healthy controls and 6 ACS patients. The datasets were generated using different detection platforms. GSE94605 was based on the 'miRCURY LNA microRNA Array, sixth generation—hsa, mmu and rno' platform, GSE60993 used the 'Illumina HumanWG-6 v3.0 Expression BeadChip' and GSE61144 was derived from the 'Sentrix Human-6 v2 Expression BeadChip'. GSE60993/GSE61144 samples from patients with ACS who visited the emergency department within 4 h after the onset of chest pain. GSE60993 did not include specific information about sample collection time. However, detailed demographic and clinical information (e.g., age, sex and comorbidities) was not provided by the original contributors. Therefore, this information could not be incorporated into our analysis and represents a limitation of the study.

The GSE60993 and GSE94605 datasets were used to identify differentially expressed genes (DEGs) and differentially expressed miRNAs (DEMs), respectively, whereas the GSE61144 dataset was used to validate DEGs expression. The standardized expression matrices and sample annotation information for these datasets are available for download and analysis from the GEO database.

During data preprocessing, we examined the distribution of each dataset to assess whether the downloaded expression matrices were standardized. This was done by referencing the GEO2R script and evaluating quartile distributions. If the data were not already log-transformed, a log2 transformation was applied. For this study, the selected datasets provided pre-normalized expression matrices. To evaluate data quality and sample consistency, we checked expression distributions using boxplots and assessed sample clustering through dimensionality reduction with UMAP and t-SNE (Supporting Information S2).

2.2 | Differential Expression Analysis

Differential expression analysis was conducted using R package 'limma', identifying DEGs and DEMs by comparing acute coronary syndrome (ACS) patients with normal controls in the GSE60993 and GSE94605 datasets, respectively. The criteria for screening DEGs were $p < 0.05$ and $|\log FC| \geq 0.8$, whereas the criteria for DEMs were $p < 0.05$ and $|\log FC| \geq 1$. Visualisation of DEGs/DEMs was performed using the R package 'ggplot2' and 'pheatmap'.

2.3 | Functional Gene Enrichment Analysis

The R package 'clusterProfiler' was used to perform Gene Ontology (GO)—covering biological processes, cellular components and molecular functions—as well as KEGG on DEGs. Pathways were considered significant if $p < 0.05$. The results were visualised using bar charts created using the R package 'ggplot2'.

Additionally, 'clusterProfiler' was employed to conduct gene set enrichment analysis (GSEA) to identify enriched gene sets. Reference gene sets 'h.all.v2024.1. Hs.symbols.gmt' and 'c2. cp.kegg_legacy.v2024.1. Hs.symbols.gmt' were downloaded from the MSigD (https://www.gsea-msigdb.org/gsea/msigdb/). Screening criteria for significant gene sets were $|NES| > 1$ and a $p < 0.05$. The R package 'enrichplot' was used to visualise the trend changes in the GSEA pathways.

2.4 | Screening for Genes

The miRDIP database (https://ophid.utoronto.ca/mirDIP/) was utilised to predict potential target genes of miRNAs, with the screening criterion set to a minimum score of 'very high'. Genes that overlapped between predicted target genes, DEGs and key module identified through weighted gene co-expression network analysis (WGCNA) were selected for further screening. The interaction network of DEMs and their associated genes was visualised by Cytoscape (v3.10.2).

2.5 | Machine Learning

LASSO and SVM-RFE algorithms were employed to identify potential biomarkers for ACS. LASSO, introduces a penalty coefficient (λ) to optimise the model by reducing gene dimensionality. SVM-RFE, on the other hand, is a linear classifier that uses supervised learning to perform binary classification of data. The R packages 'glmnet' and 'caret' were used for LASSO and SVM-RFE analysis, respectively, and the genes identified by both algorithms were regarded as candidate biomarkers for ACS. Specifically, in the LASSO analysis, we used the glmnet () function from the glmnet package, with the family parameter set to 'binomial.' For SVM-RFE, we employed the rfe () function from the caret package, setting the method to 'svmLinear' and using 3-fold cross-validation, which was selected due to the limited sample size. Unless otherwise stated, default parameters were used in the R packages. Receiver operating characteristic (ROC) curves were calculated to evaluate the diagnostic utility, with genes having an AUC > 0.7 selected.

2.6 | Evaluation of Immune Cell Subtype Composition

CIBERSORT is a deconvolution algorithm that employs support vector regression to analyse the expression matrix of human immune cell subsets. The CIBERSORT. R script and the immune cell expression matrix were obtained from the CIBERSORT website (https://cibersortx.stanford.edu/). The R package 'ggplot2' was used to create stacked bar charts, illustrating the relative percentages of cell subsets and box plots to visualise the differences in the proportions of cell subtypes between the normal and ACS groups. Pearson correlation was performed to assess the association between biomarker expression and each immune cell type in ACS, with lollipop charts generated using 'ggplot2' to present the results.

2.7 | Statistical Analysis

Statistical analyses and data visualisation were performed using R (v 4.4.0) and GraphPad Prism (version 9.0.0). The Students' *t*-test was used to assess significant differences in biomarker expression. Pearson correlation evaluated the relationship. $p < 0.05$ was considered statistically significant.

3 | Results

3.1 | Identification of DEGs

Data sample distribution and gene expression characteristics are visualised using scatter plots and box plots, respectively (Supporting Information S1: Figure S1–S3). In the GSE60993 dataset, 98 DEGs were confirmed between the ACS and normal groups, comprising 70 increased and 20 decreased mRNAs as shown in the volcano and heatmap plot (Figure 1A,B). In the GSE94605 dataset, 627 DEMs were found, containing 352 elevated and 275 reduced miRNAs as shown in the volcano and heatmap plot (Figure 1C,D). The volcano plot illustrates the overall distribution of differentially expressed genes, whereas the heatmap displays the expression changes. The details of DEGs and DEMs are in Table S1.

3.2 | Functional Enrichment Analysis

The GO results of the upregulated and downregulated differentially expressed mRNAs were shown in Figure 2A,B, respectively. GO analysis revealed that in the biological process (BP) category, upregulated DEGs were primarily enriched in inflammatory response and immune regulation (GO:0042742, GO:0032496, GO:0002237, GO:0001818, GO:0019730, GO:0001906, GO:0031640, GO:0141061 and GO:0141060), whereas downregulated DEGs were mainly associated with immune-related processes (GO:0002399, GO:0002503, GO:0002396, GO:0002501, GO:0019886, GO:0002495, GO:0002504, GO:0002478, GO:-0002449 and GO:0019884). Regarding cellular components (CC), upregulated DEGs were predominantly enriched in pathways related to granular lumen/membrane and vesicle lumen (GO:0035580, GO:0034774, GO:0060205, GO:0031983, GO:1904724, GO:0030667, GO:0070821 and GO:0035579), whereas downregulated mRNAs were enriched in immune response and vesicle-related pathways (GO:0042613, GO:0042611, GO:0030669, GO:0071753, GO:0045334, GO:0005770, GO:0030139 and GO:0030665). In the molecular function category (MF), upregulated DEGs were enriched in pathways related to protease activity and receptor activity (GO:0016813, GO:0016810, GO:0140375, GO:0038187,

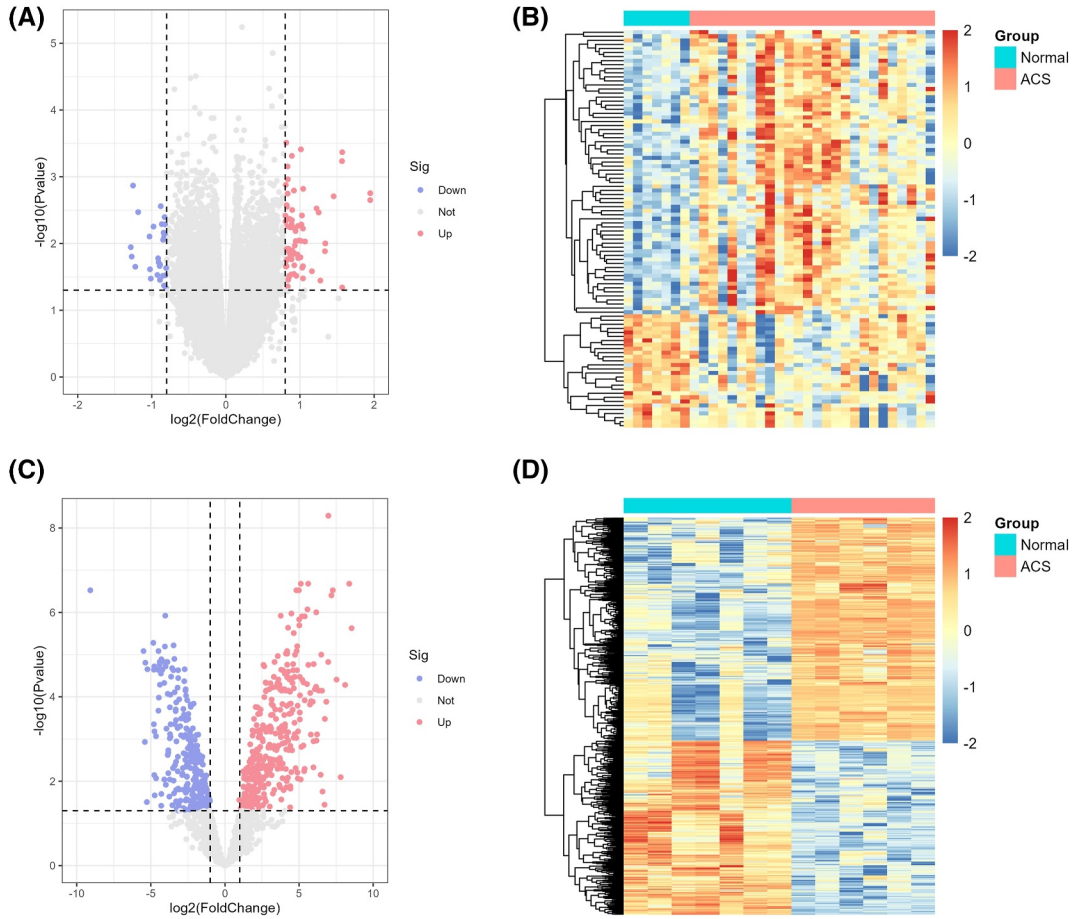

FIGURE 1 | Differential expression analysis of mRNA and miRNA (ACS vs. normal). (A, B) The volcano plot (A) and heatmap (B) of DEGs in GSE60993. (C, D) The volcano plot (C) and heatmap (D) of DEMs in GSE94605. ACS: acute coronary syndrome; DEG: differentially expressed gene; DEMs: differentially expressed miRNAs.

GO:0140313, GO:0016836, GO:0008235 and GO:0008237), whereas downregulated DEGs were primarily involved in regulating immune receptor activity and peptide binding pathways (GO:0140375, GO:0023023, GO:0032395, GO:0003823, GO:0023026, GO:0042605 and GO:0042277) (Figure 2A,B). The details of GO analysis are in Table S2.

KEGG analysis indicated that upregulated DEGs were enriched in pathways associated with the immune system and small molecule metabolism (hsa00480, hsa04920, hsa04613, hsa04657, hsa04640 and hsa00730) (Figure 2C). Downregulated DEGs were linked to pathways related to the immune system and immune diseases (hsa05332, hsa04612, hsa04658, hsa04640 and hsa04659) (Figure 2D). The bar chart displays the top 10 pathways identified in the three GO categories and the KEGG enrichment analysis. The details of KEGG analysis are in Table S2.

The top five enriched pathways from both the HALLMARK and KEGG gene sets were shown in Figure 3A,B, respectively. The GSEA enrichment results indicated that all pathways enriched in the GSE60993 dataset were activated in the ACS group. Within the hallmark gene set, the enriched pathways primarily include MYC targets, the MTORC1 signalling pathway and oxidative phosphorylation (Figure 2E). In the KEGG gene set, the activated pathways mainly encompass the T cell receptor signalling pathway, primary immunodeficiency, ribosome biogenesis and cell adhesion molecules, among others (Figure 2F). The details of GSEA are in Table S2.

3.3 | Identification of Key Modules by WGCNA

In this study, WGCNA was applied to discover gene modules tightly connected to ACS in the GSE60993. With the soft threshold set to 12, the scale-free fit index reached 0.9 (Figure 3A). A total of 36 co-expression modules were identified through hierarchical clustering (Figure 3B). The green module, which contained 1050 genes, exhibited the highest absolute correlation (Figure 3C). Additionally, the scatter plot indicated a notable positive correlation between the relationships of genes and modules and the relationships of genes and traits (Figure 3D), leading us to focus on this module for further analysis.

3.4 | Screening for Genes and Construction of the miRNA–mRNA Network

Using miRDIP for integration, the miRNA–mRNA targeted interaction network was constructed. According to the predictions made by miRDIP, 11,285 genes were recognized as potential targets of 627 differentially expressed miRNAs. 14 genes were isolated from the potential target, DEGs and WGCNA green

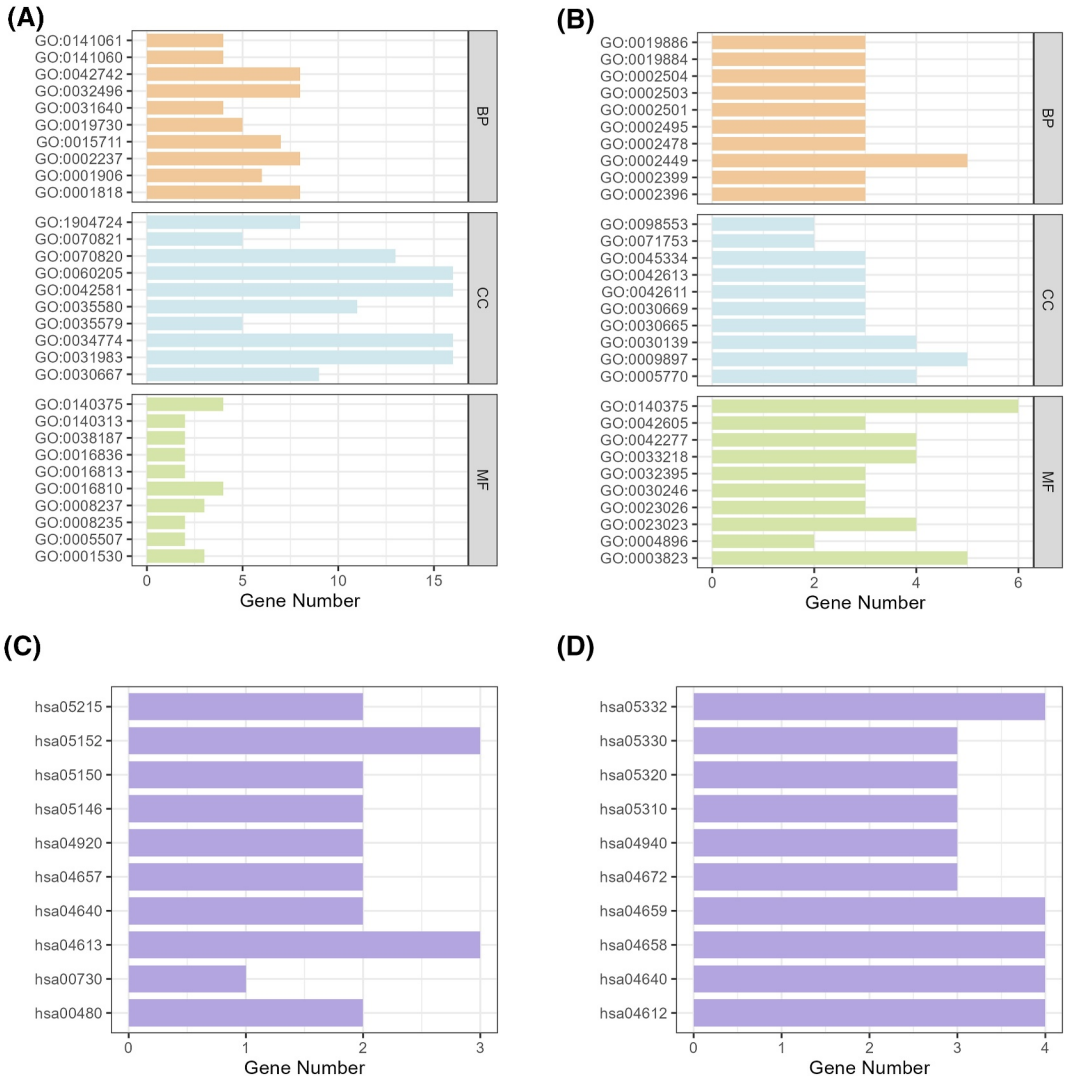

FIGURE 2 | Pathway enrichment analysis. (A, B) GO analysis (top 10) of the increased (A) and decreased DEGs (B). (C, D) KEGG analysis (top 10) of the elevated (C) and reduced DEGs (D). (E, F) GSEA revealed the top five enrichment pathways activated in ACS using hallmark gene sets (E) and KEGG gene sets (F). ACS: acute coronary syndrome; DEGs: differentially expressed genes; DEMs: differentially expressed miRNAs; GO: gene ontology; GSEA: gene set enrichment analysis; KEGG: kyoto encyclopaedia of genes and genomes.

model (Figure 4A). Subsequently, these 14 genes and their predicted targeting relationships from miRDIP were further analysed to refine the miRNA-–mRNA network. Following the analysis of expression trends in the differentially expressed genes, 1 gene and its targets were excluded. The miRNA–mRNA network including 40 pairs was constructed, comprising 36 DEMs and 13 upregulated DEGs (Figure 4B).

3.5 | Diagnostic Performance of Biomarkers

To identify biomarkers associated with ACS, we employed 2 algorithms to evaluate characteristic genes based on the 13 DEGs. The LASSO and SVM-RFE identified 3 and 7 genes as characteristic, respectively (Figure 4C,D). The intersection of the genes identified by both algorithms yielded three common genes—ARG1, HECW2 and PFKFB3—which were proposed as candidates for ACS (Figure 4E). The ROC curve analysis revealed that the AUC values for these 3 genes were all above 0.8, suggesting their strong diagnostic efficacy in the GSE60993 dataset (Figure 5A–C). In the validation using GSE61144 (Figure 5E), the expression trends of these three genes were consistent with those observed in GSE60993 (Figure 5D), and the expression levels exhibited statistically significant differences (Figure 5D,E).

3.6 | Immune Cell Proportions in ACS and Their Correlation With Biomarkers

Figure 6A displays the relative proportions of immune cell composition across all samples based on the CIBERSORT.

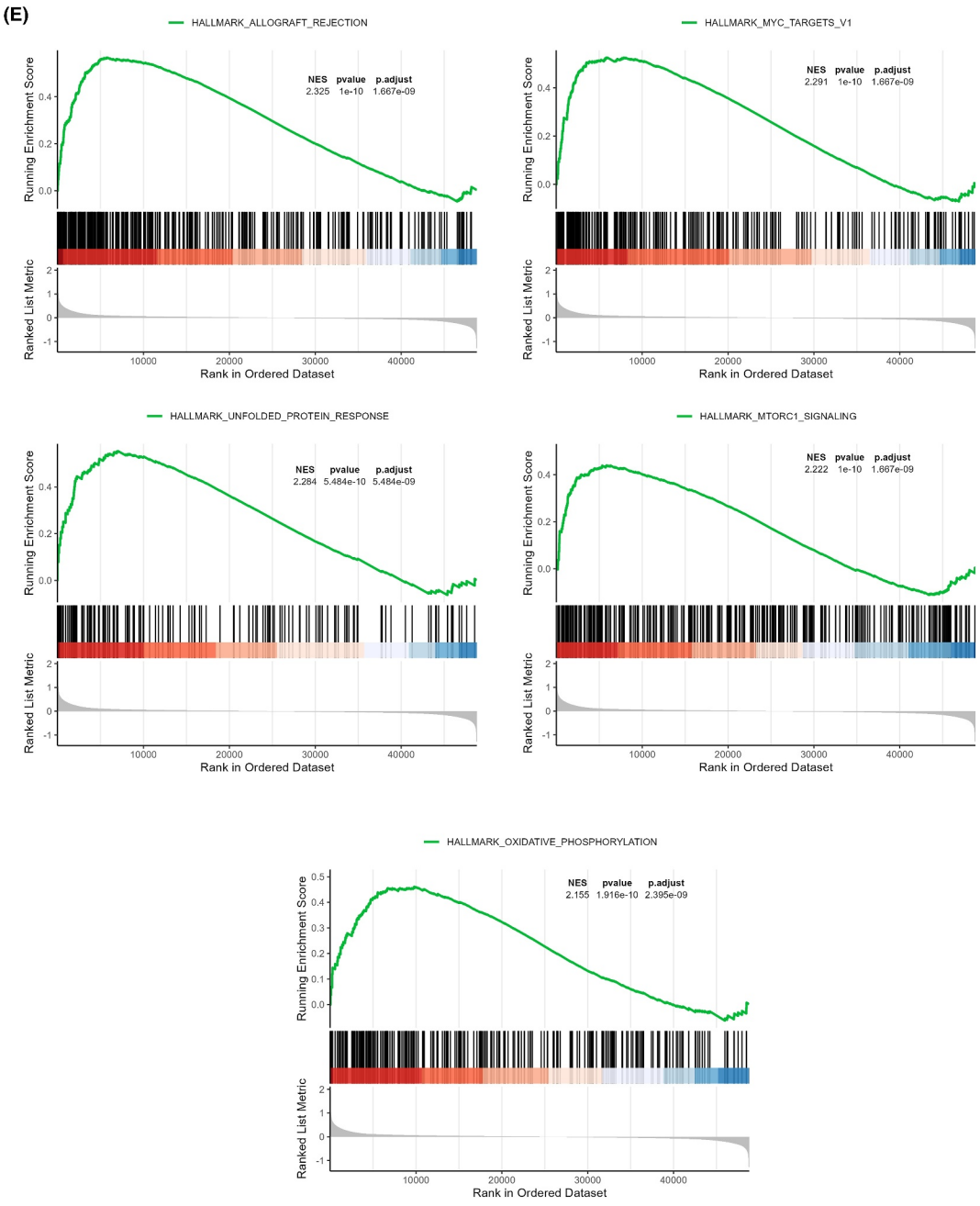

FIGURE 2 | (Continued)

Compared to the normal, 3 cell subtypes showed significant changes in the ACS group: the fraction of resting memory CD4 T cells was downregulated, whereas the proportions of monocytes and neutrophils were upregulated (Figure 6B).

ARG1 significantly positively correlated with neutrophils and M0 macrophages, whereas negatively correlated with CD8 T cells. HECW2 exhibited a significant positive relationship with neutrophils and M0 macrophages, alongside a significant negative link with gamma delta T cells and memory B cells. Similarly, PFKFB3 was positively correlated with neutrophils and M0 macrophages but negatively associated with CD8 T cells and memory B cells (Figure 6C).

4 | Discussion

ACS imposes a significant economic burden on families. With an ageing demographic, the prevalence of ACS is forecasted to rise annually [19]. The characteristic of ACS is a sudden onset and progresses rapidly, even leading to severe and life-threatening complications [20]. Understanding the mechanisms underlying ACS is crucial for facilitating early diagnosis and timely treatment, ultimately helping to reduce complications and improve prognosis. The untimely activation of immune inflammation promotes the worsening of ACS [21]. Identifying specific pathways and biomarkers related to immune inflammation could inform effective treatment and recovery strategies for ACS. This

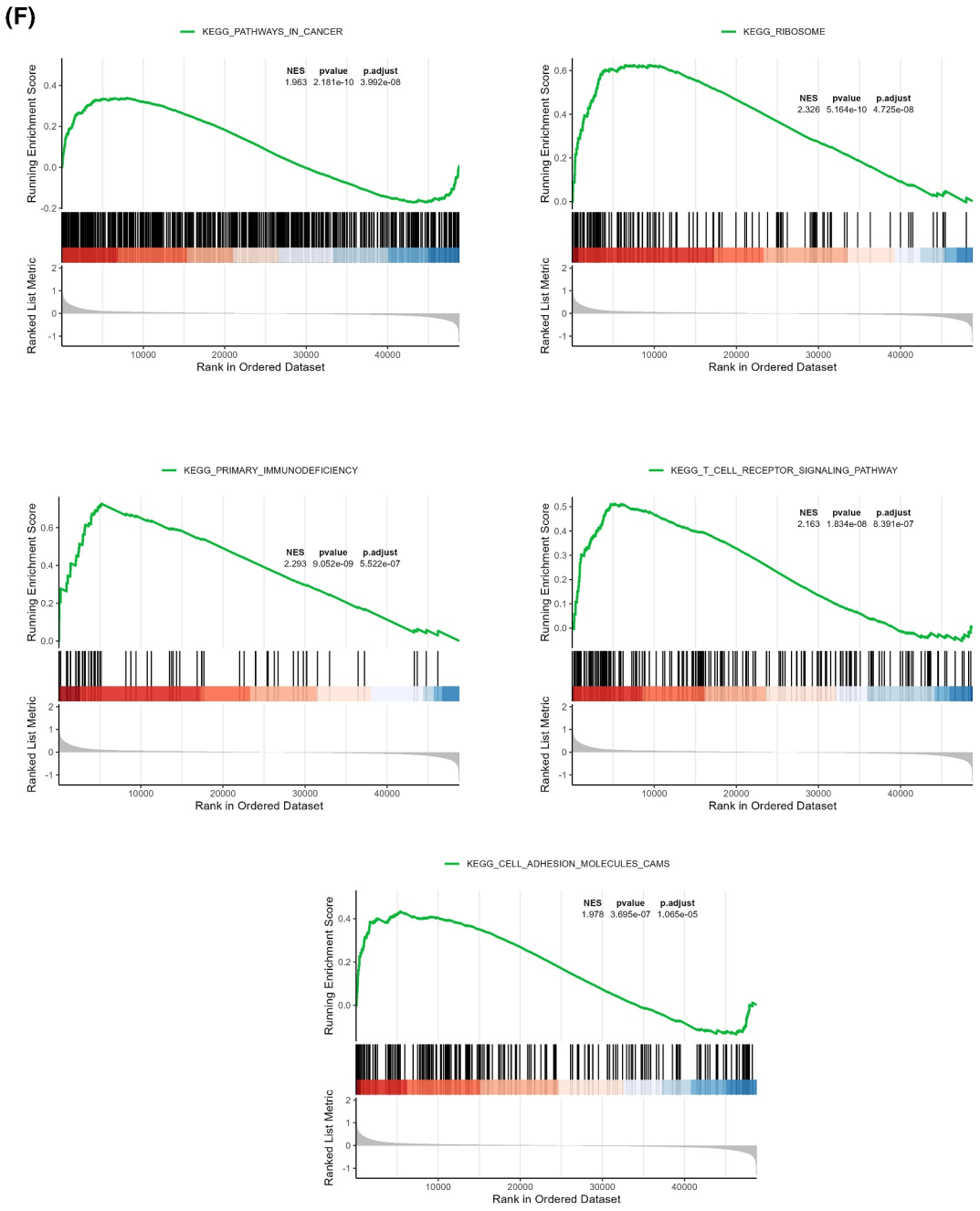

FIGURE 2 | (Continued)

study utilised public sequencing data to construct a miRNA–mRNA interaction network associated with ACS, conducted bioinformatics analyses to explore its pathological processes and identified marker genes using WGCNA and machine learning.

ACS represents the most severe manifestation of coronary atherosclerotic heart disease in its advanced stages [22]. Current research studies indicate that various immune cells play critical roles in the development of atherosclerosis. Besides lipid deposits, arterial plaques harbour diverse immune infiltrating cells, including neutrophils, T cells and macrophages [9]. Studies have linked dilated cardiomyopathy to resting CD4 memory T cells [23]. Neutrophils, known for secreting proinflammatory mediators, are elevated in the serum of coronary artery disease, aligning with our findings [24]. Additionally, the levels of monocytes increased, which are significant contributors to inflammatory processes, including atherosclerosis. Notably, their rise post-myocardial infarction correlates with poor recovery and adverse prognosis [25]. The CIBERSORT analysis revealed significant changes in immune cell proportions, particularly involving neutrophils, monocytes and CD4+ T cells. The increased proportions of neutrophils and monocytes likely reflect the acute inflammatory state during plaque rupture, promoting thrombosis and tissue injury. Conversely, reduced memory CD4+ T cells may impair adaptive immunity and vascular repair. This immune shift suggests a

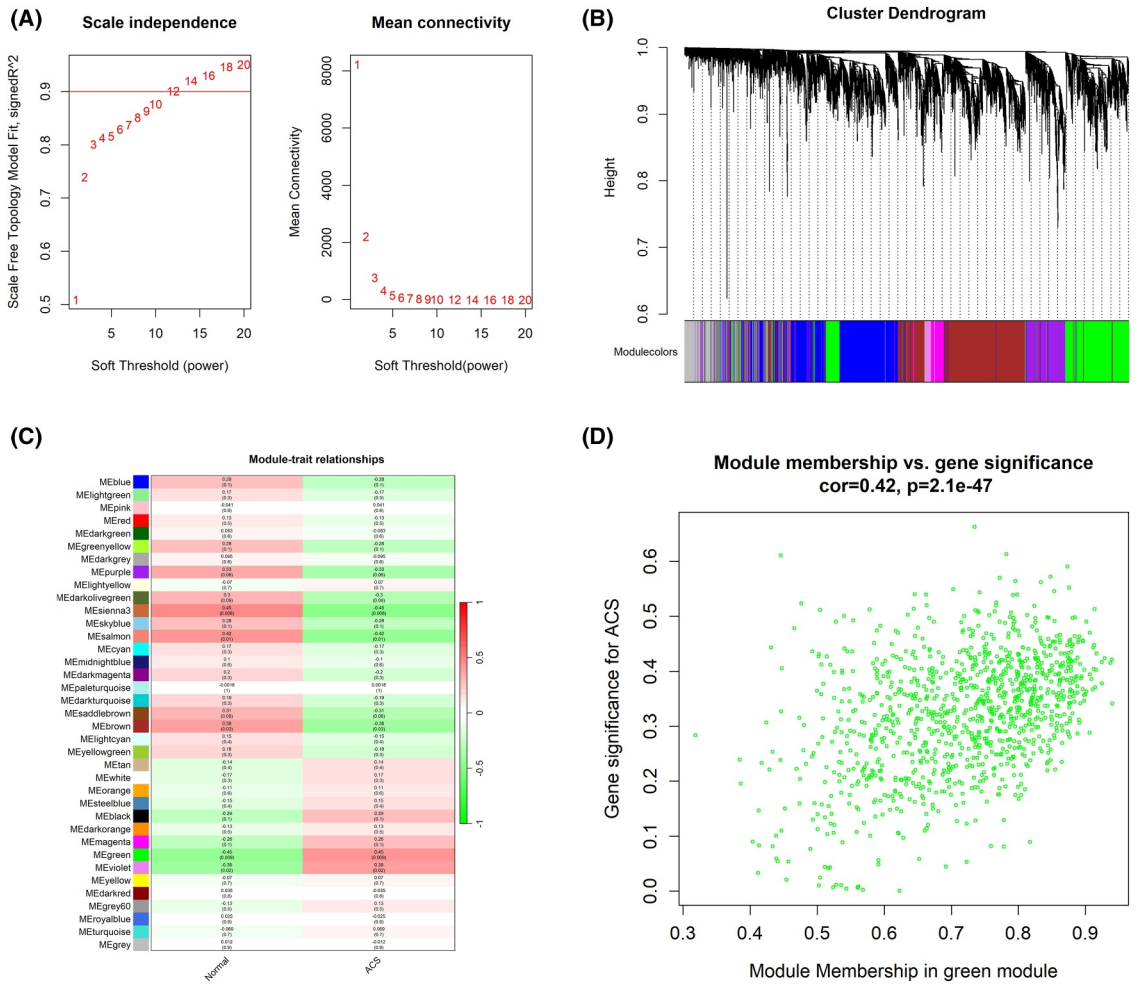

FIGURE 3 | WGCNA analysis of GSE60993. (A) Soft threshold power screening and construction of a scale-free network. (B) Clustering dendrogram. (C) Correlation heatmap between module eigengenes and clinical traits. (D) The correlation between module membership versus ACS gene significance in the green module. ACS: acute coronary syndrome; WGCNA: weighted gene co-expression network.

dysfunctional response that exacerbates disease severity [26]. The GSEA results revealed that immune-inflammation-related pathways, such as T cell receptor signalling and primary immune deficiency, were enriched in the ACS. Furthermore, the enrichment pathways, including cell adhesion molecules, MYC targets and MTORC1 signalling, were observed. The relationship between the immune response and these pathways is well-documented in the context of ACS progression [27–29], suggesting that treatments designed for immune-inflammatory responses may hold considerable promise for the management of ACS.

Assessing the patterns of gene expression can deliver new understandings of ACS mechanisms and assist in identifying intervention focuses. This study identified a module associated with ACS using WGCNA. Through bioinformatics analysis, machine learning, and external data validation, ARG1, HECW2 and PFKFB3 were identified as promising biomarkers for ACS.

ARG1 is distributed in endothelial cells, vascular smooth muscle cells and specific immune cell populations [30]. Increased arginase activity disrupts nitric oxide synthase (NOS) function, causing NOS dimers to uncouple, which can contribute to diabetic cardiovascular dysfunction [31]. The elevated ARG1 expression and arginase activity have been linked to vascular dysfunction in vitro models of diabetic vascular disease [32, 33]. Upregulation of ARG1 expression has been observed in ACS, aligning with our findings [34]. Furthermore, ARG1 has been identified as a biomarker for disease progression in atrial fibrillation (the complication associated with COVID-19) and shows a positive correlation with neutrophil levels [35]. Additionally, when simvastatin was used to treat atherosclerosis by targeting macrophages and reducing local inflammation, ARG1 expression was found to be synchronously downregulated [36]. The ARG1 rs2781666 polymorphism is associated with increased common carotid artery intima-media thickness, indicating a significant role of ARG1 in vascular pathophysiology [37].

PFKFB3 is a crucial glycolytic enzyme that drives macrophage and endothelial cell activation and inflammation [38]. It is reported that its expression is elevated following myocardial infarction and is closely linked to chemokine signalling, as well as immune and inflammatory responses [39]. High levels of PFKFB3 are associated with the vulnerability of atherosclerotic plaques both in humans and mice, and inhibiting PFKFB3 activity in mouse models has been shown to enhance plaque stability [40]. Furthermore, the phenotypic transformation of

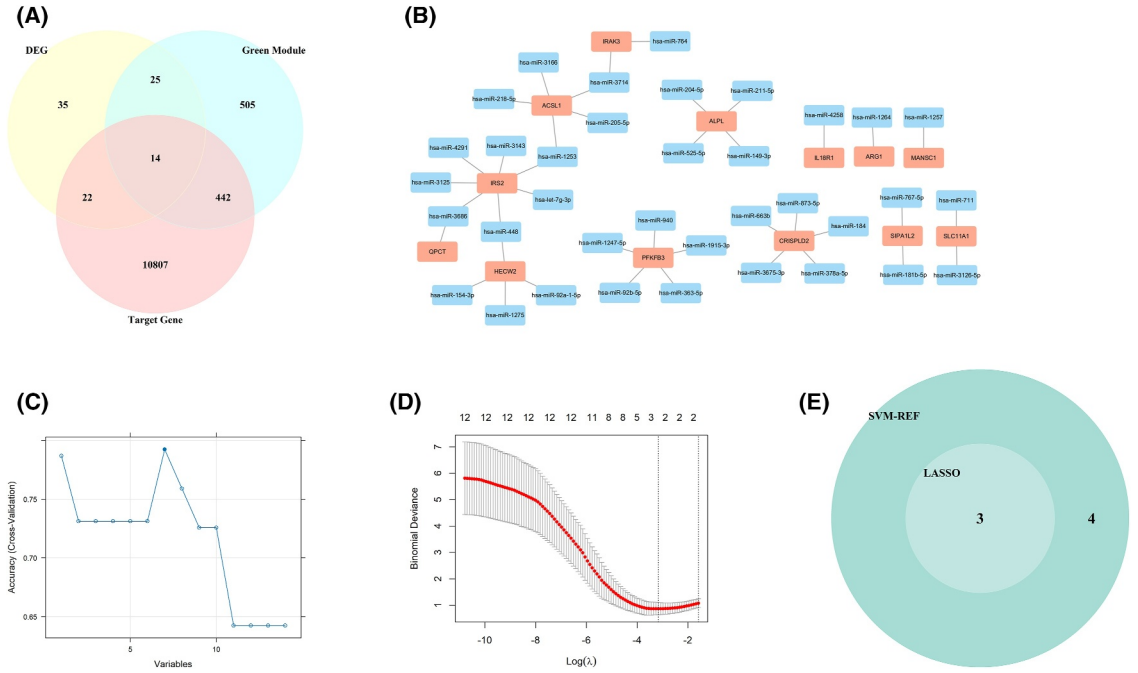

FIGURE 4 | Screening biomarkers in ACS using machine learning. (A) The intersection of the DEGs, green module, and prediction targets of DEMs. (B) The miRNA–mRNA network by Cytoscape. (C) The LASSO regression identified 3 genes. (D) The SVM-RFE algorithm identified 7 genes. (E) 3 genes were extracted from the intersection of 2 algorithms. ACS: acute coronary syndrome; DEGs: differentially expressed genes; LASSO: least absolute shrinkage and selection operator; RMSE: root mean square error; SVM-RFE: support vector machine-recursive feature elimination.

smooth muscle cells in atherosclerotic lesions is closely linked to glycolysis, particularly the abnormal expression of PFKFB3 [41]. Under hypoxia-induced conditions, the PFKFB3/NLRP3 regulatory axis plays a crucial role in macrophage inflammatory activation [42]. However, another study revealed that although PFKFB3 deficiency reduced atherosclerosis in mice, complete loss of PFKFB3 exacerbated disease progression due to compromised macrophage function [43]. This suggests that PFKFB3 acts as a double-edged sword, highlighting the need for caution when developing antiatherosclerotic therapies targeting this enzyme.

HECW2 was initially identified as a biomarker for ACS. In research focusing on circRNA screening, the circRNA has-circ-0118464, which corresponds to the HECW2 gene, showed significant upregulation in individuals with heart failure [44]. HECW2 encodes the E3 ubiquitin ligase family members, playing a critical role in angiogenesis by stabilising connections between endothelial cells [45]. In colorectal cancer, HECW2 has been implicated in promoting tumour development and chemotherapy resistance [46]. Additionally, mutations in HECW2 have been associated with neurological disorders such as intellectual disability and neurodevelopmental delays [47]. The HECW2 levels have also been linked to alterations in immune response cell populations in liver cancer [48]. Similarly, HECW2 was screened as an immune-related hub gene in ischaemic stroke [49].

Interestingly, all three biomarkers are implicated in both immune regulation and metabolic processes. ARG1 and PFKFB3 have been linked to macrophage polarization, although HECW2 plays a role in protein ubiquitination that influences immune cell signalling and has also been identified as an immune-related hub gene. This convergence suggests these genes may act within a shared immunometabolic axis influencing ACS pathology. Based on these results, it is suggested that ARG1, HECW2 and PFKFB3 are potential biomarker candidates in ACS. Further comprehensive studies, particularly focusing on their functions in immune response, are warranted.

This study has several limitations. Although the biomarkers ARG1, HECW2 and PFKFB3 were identified and found to be closely associated with specific immune cells, no in-depth analyses were conducted to explore further the complex interactions between these genes and immune cell populations. Additionally, although a miRNA–mRNA network encompassing 36 miRNAs was constructed, further investigation into these miRNAs, such as verifying expression trends or performing dual luciferase assays to confirm interactions with mRNA, was not undertaken. The validation of the screened mRNA relied solely on public sequencing data, without collecting clinical samples for further confirmation, and animal experiments were not performed to study changes in gene expression. This approach may introduce potential errors associated with high-throughput sequencing data. Therefore, the findings require further verification through in vitro and in vivo assays. Future research studies will aim to validate the diagnostic value of these biomarkers using RT-qPCR and immunohistochemistry/WB in ACS patient cohorts. We also plan to employ deep learning frameworks, such as convolutional neural networks or autoencoders [50–52], to model nonlinear interactions between gene expression and immune phenotypes, potentially revealing additional biomarkers. Emerging deep learning models, such as convolutional neural networks, graph neural networks and autoencoders, offer powerful tools for high-dimensional transcriptomic data analysis [53, 54]. Future studies may integrate these methods to refine biomarker selection and uncover novel regulatory networks in ACS.

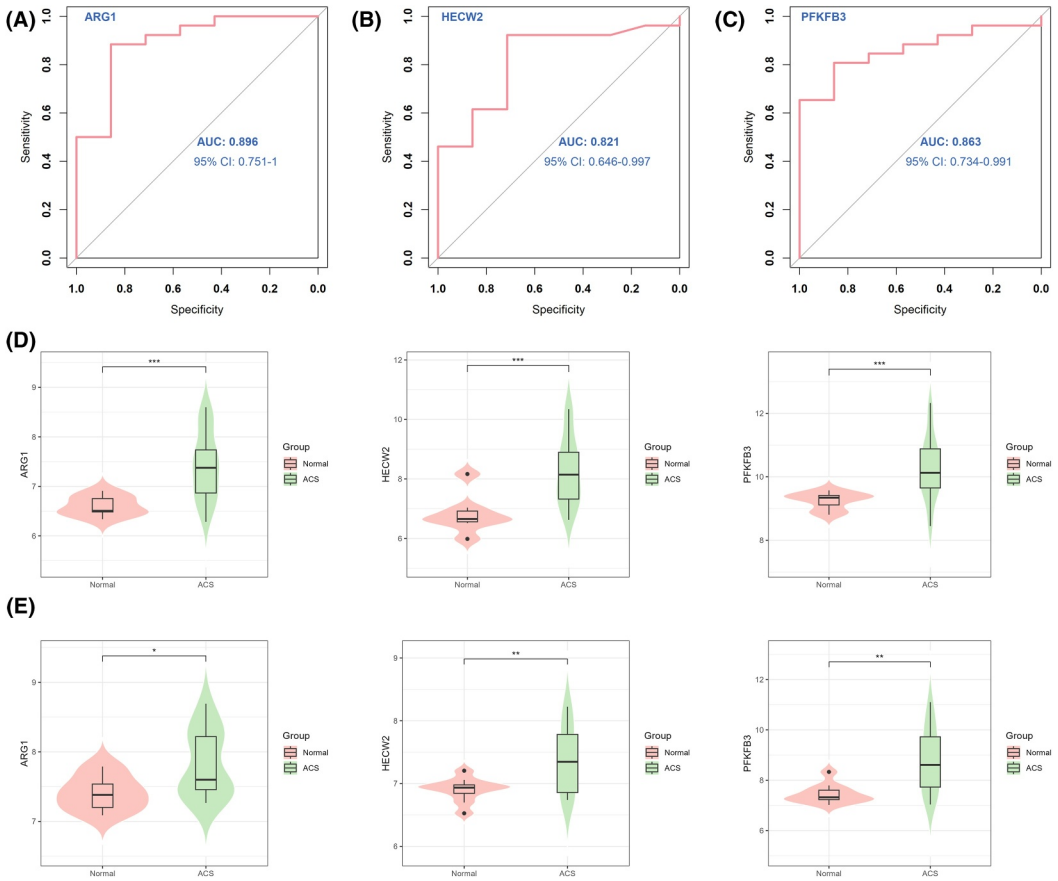

FIGURE 5 | Diagnostic performance and validation of biomarkers levels. (A-C) ROC curve analysis of ARG1 (A), HECW2 (B) and PFKFB3 (C) in GSE60993. (E, F) The levels of ARG1, HECW2, and PFKFB3 in GSE60993 (E) and GSE61144 (F). ACS: acute coronary syndrome; AUC: area under the ROC curve; ROC, receiver operating characteristic. *$p < 0.05$, **$p < 0.01$, ***$p < 0.0001$.

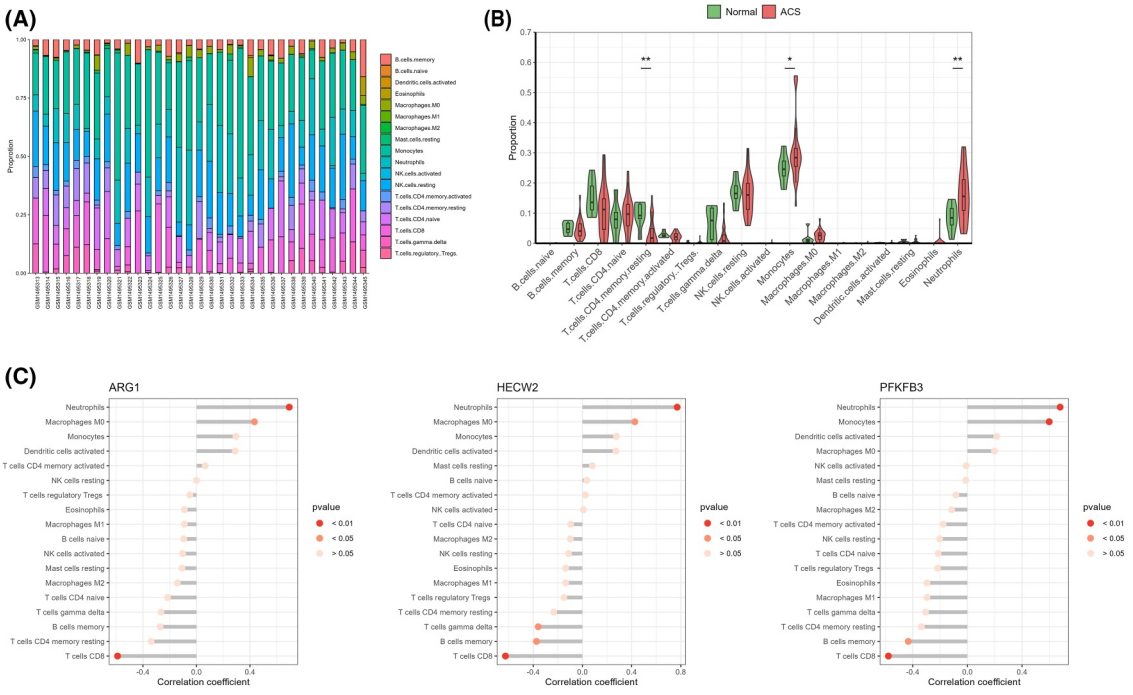

FIGURE 6 | Quantification of immune cell subtypes in GSE60993. (A) The relative composition of the immune cell. (B) Different fractions of immune cell subsets in ACS and normal. (C) The correlation between biomarkers and immune cell subtypes. ACS: acute coronary syndrome. *$p < 0.05$, **$p < 0.01$.

5 | Conclusion

In summary, three biomarkers for ACS were identified: ARG1, HECW2 and PFKFB3. Enrichment analysis revealed functional pathways linked to the immune-inflammatory response in ACS. Including the neutrophils and monocytes, the proportions of various immune cell subtypes were altered. ARG1, HECW2 and PFKFB3 are related to specific immune cells, and further investigation of these genes may uncover new therapeutic targets for ACS.

Author Contributions

conceptualization: J.Z., F.G., L.Z., Y.Z. data curation: J.Z., F.G., L.Z., Y. Z. formal analysis, L.Z., Y.Z. funding acquisition: Y.Z. investigation: L. Z., Y.Z. methodology: J.Z., F.G., L.Z., Y.Z. project administration: Y.Z. resources: L.Z. software: L.Z., Y.Z. supervision: Y.Z. validation: L.Z. visualization: L.Z. roles/writing – original draft: L.Z. writing – review and editing: J.Z., F.G., Y.Z.

Ethics Statement

The authors have nothing to report.

Consent

The authors have nothing to report.

Conflicts of Interest

The authors declare no conflicts of interest.

Data Availability Statement

The data that support the findings of this study are available from the corresponding author upon reasonable request.

References

1. R. Dizaji, H. Zarei, R. Miri, M. Yousefifard, and M. Yousefifard, "Performance of Manchester Acute Coronary Syndromes Decision Rules in Acute Coronary Syndrome: A Systematic Review and Meta-Analysis," *European Journal of Emergency Medicine: Official Journal of the European Society For Emergency Medicine* 31, no. 5 (2024): 310–323, https://doi.org/10.1097/MEJ.0000000000001147.

2. W.-Bo Dai, J.-Yi Ren, Su-T. Hu, et al., "The Safety and Efficacy of Indobufen or Aspirin Combined With Clopidogrel in Patients With Acute Myocardial Infarction After Percutaneous Coronary Intervention," *Platelets* 35, no. 1 (2024): 2364748, https://doi.org/10.1080/09537104.2024.2364748.

3. Y. Asada, A. Yamashita, Y. Sato, and K. Hatakeyama, "Pathophysiology of Atherothrombosis: Mechanisms of Thrombus Formation on Disrupted Atherosclerotic Plaques," *Pathology International* 70, no. 6 (2020): 309–322, https://doi.org/10.1111/pin.12921.

4. E. D. Grech and D. R. Ramsdale, "Acute Coronary Syndrome: Unstable Angina and Non-ST Segment Elevation Myocardial Infarction," *BMJ* 326, no. 7401 (2003): 1259–1261, https://doi.org/10.1136/bmj.326.7401.1259.

5. D. L. Bhatt, R. D. Lopes, and R. A. Harrington, "Diagnosis and Treatment of Acute Coronary Syndromes: A Review," *JAMA* 327, no. 7 (2022): 662–675, https://doi.org/10.1001/jama.2022.0358.

6. Writing Committee of the Report on Cardiovascular Health and Diseases in China, "Report on Cardiovascular Health and Diseases in China 2021: An Updated Summary," *Biomedical and Environmental Sciences: Biomedical and Environmental Sciences* 35, no. 7 (2022): 573–603, https://doi.org/10.3967/bes2022.079.

7. Y. Wu, Z. Shi, X. Zhou, et al., "Schicyclepred: A Deep Learning Framework for Predicting Cell Cycle Phases From Single-Cell Hi-C Data Using Multi-Scale Interaction Information," *Communications Biology* 7, no. 1 (2024): 923, https://doi.org/10.1038/s42003-024-06626-3.

8. M. P. G. Leers, C. Stockem, D. Ackermans, et al., "Intermediate and Nonclassical Monocytes Show Heterogeneity in Patients With Different Types of Acute Coronary Syndrome," *Cytometry Part A: The Journal of the International Society for Analytical Cytology* 91, no. 11 (2017): 1059–1067, https://doi.org/10.1002/cyto.a.23263.

9. M. C. Flynn, G. Pernes, M. K. S. Lee, P. R. Nagareddy, and A. J. Murphy, "Monocytes, Macrophages, and Metabolic Disease in Atherosclerosis," *Frontiers in Pharmacology* 10 (2019): 666, https://doi.org/10.3389/fphar.2019.00666.

10. K. J. Woollard and G. Frederic, "Monocytes in Atherosclerosis: Subsets and Functions," *Nature Reviews Cardiology* 7, no. 2 (2010): 77–86, https://doi.org/10.1038/nrcardio.2009.228.

11. M. Katsioupa, I. Kourampi, E. Oikonomou, et al., "Novel Biomarkers and Their Role in the Diagnosis and Prognosis of Acute Coronary Syndrome," *Life (Basel, Switzerland)* 13, no. 10 (2023): 1992, https://doi.org/10.3390/life13101992.

12. Y. Zhao, X. Song, Y. Ma, X. Liu, and Y. Peng, "Circulating mir-483-5p as a Novel Diagnostic Biomarker for Acute Coronary Syndrome and Its Predictive Value for the Clinical Outcome After PCI," *BMC Cardiovascular Disorders* 23, no. 1 (2023): 360, https://doi.org/10.1186/s12872-023-03387-5.

13. R. M. O'Connell, K. D. Taganov, M. P. Boldin, G. Cheng, and D. Baltimore, "MicroRNA-155 Is Induced During the Macrophage Inflammatory Response," *Proceedings of the National Academy of Sciences of the United States of America* 104, no. 5 (2007): 1604–1609, https://doi.org/10.1073/pnas.0610731104.

14. M. Ceppi, P. M. Pereira, I. Dunand-Sauthier, et al., "MicroRNA-155 Modulates the Interleukin-1 Signaling Pathway in Activated Human Monocyte-Derived Dendritic Cells," *Proceedings of the National Academy of Sciences of the United States of America* 106, no. 8 (2009): 2735–2740, https://doi.org/10.1073/pnas.0811073106.

15. Y. Fang, C. Shi, E. Manduchi, M. Civelek, and P. F. Davies, "MicroRNA-10a Regulation of Proinflammatory Phenotype in Athero-Susceptible Endothelium in vivo and in VITRO," *Proceedings of the National Academy of Sciences of the United States of America* 107, no. 30 (2010): 13450–13455, https://doi.org/10.1073/pnas.1002120107.

16. K. Chandan, M. Gupta, and M. Sarwat, "Role of Host and Pathogen-Derived Micrornas in Immune Regulation During Infectious and Inflammatory Diseases," *Frontiers in Immunology* 10 (2019): 3081, https://doi.org/10.3389/fimmu.2019.03081.

17. Li-J. Chen, S. H. Lim, Yi-T. Yeh, S.-C. Lien, and J.-J. Chiu, "Roles of Microrna in Atherosclerosis and Restenosis," *Journal of Biomedical Science* 19, no. 1 (2012): 79, https://doi.org/10.1186/1423-0127-19-79.

18. A. R. R. Forrest, M. Kanamori-Katayama, Y. Tomaru, et al., "Induction of Microrna, mir-155, mir-222, mir-424 and mir-503, Promotes Monocytic Differentiation Through Combinatorial Regulation," *Leukemia* 24, no. 2 (2010): 460–466, https://doi.org/10.1038/leu.2009.246.

19. V. Di, F. Di Giusto, S. Mazzotta, et al., "Management of Vulnerable Patient Phenotypes and Acute Coronary Syndrome Mechanisms," *International Journal of Cardiology* 415 (2024): 132365, https://doi.org/10.1016/j.ijcard.2024.132365.

20. D. E. Jones, M. Braun, and D. Kassop, "Acute Coronary Syndrome: Common Complications and Conditions That Mimic ACS," *FP Essentials* 490 (2020): 29–34.

21. G. Cimmino, F. S. Loffredo, A. Morello, et al., "Immune-Inflammatory Activation in Acute Coronary Syndromes: A Look Into the Heart of

Unstable Coronary Plaque," *Current Cardiology Reviews* 13, no. 2 (2017): 110–117, https://doi.org/10.2174/1573403X12666161014093812.

22. H. C. Stary, A. B. Chandler, R. E. Dinsmore, et al., "A Definition of Advanced Types of Atherosclerotic Lesions and a Histological Classification of Atherosclerosis. A Report From the Committee on Vascular Lesions of the Council on Arteriosclerosis, American Heart Association," *Circulation* 92, no. 5 (1995): 1355–1374, https://doi.org/10.1161/01.cir.92.5.1355.

23. Z. Lei, J. Cao, J. Wu, Yi Lu, L. Ni, and X. Hu, "Identification of the Communal Pathogenesis and Immune Landscape Between Viral Myocarditis and Dilated Cardiomyopathy," *ESC Heart Failure* 11, no. 1 (2024): 282–292, https://doi.org/10.1002/ehf2.14585.

24. A. Zhang, W. Sun, L. Mei, et al., "Neutrophil-to-HDL-C Ratio as an Inflammatory Biomarker in Patients With Anxiety and Obstructive Coronary Artery Disease: A Retrospective Study," *Heliyon* 10, no. 19 (2024): e38829, https://doi.org/10.1016/j.heliyon.2024.e38829.

25. N. Askari, C. Lipps, S. Voss, et al., "Circulating Monocyte Subsets Are Associated With Extent of Myocardial Injury But Not With Type of Myocardial Infarction," *Frontiers in Cardiovascular Medicine* 8 (2021): 741890, https://doi.org/10.3389/fcvm.2021.741890.

26. K. Lin, S. Chen, and G. Chen, "Role of Memory T Cells and Perspectives for Intervention in Organ Transplantation," *Frontiers in Immunology* 6 (2015): 473, https://doi.org/10.3389/fimmu.2015.00473.

27. H. Harjunpää, M. L. Asens, C. Guenther, and S. C. Fagerholm, "Cell Adhesion Molecules and Their Roles and Regulation in the Immune and Tumor Microenvironment," *Frontiers in Immunology* 10 (2019): 1078, https://doi.org/10.3389/fimmu.2019.01078.

28. S. C. Casey, V. Baylot, and D. W. Felsher, "The MYC Oncogene Is a Global Regulator of the Immune Response," *Blood* 131, no. 18 (2018): 2007–2015, https://doi.org/10.1182/blood-2017-11-742577.

29. J. D. Powell, K. N. Pollizzi, E. B. Heikamp, and M. R. Horton, "Regulation of Immune Responses by Mtor," *Annual Review of Immunology* 30, no. 1 (2012): 39–68, https://doi.org/10.1146/annurev-immunol-020711-075024.

30. R. W. Caldwell, P. C. Rodriguez, H. A. Toque, S. Priya Narayanan, and R. B. Caldwell, "Arginase: A Multifaceted Enzyme Important in Health and Disease," *Physiological Reviews* 98, no. 2 (2018): 641–665, https://doi.org/10.1152/physrev.00037.2016.

31. M. J. Romero, D. H. Platt, H. E. Tawfik, et al., "Diabetes-Induced Coronary Vascular Dysfunction Involves Increased Arginase Activity," *Circulation Research* 102, no. 1 (2008): 95–102, https://doi.org/10.1161/circresaha.107.155028.

32. S. C. Elms, H. A. Toque, M. Rojas, Z. Xu, R. W. Caldwell, and R. B. Caldwell, "The Role of Arginase I in Diabetes-Induced Retinal Vascular Dysfunction in Mouse and Rat Models of Diabetes," *Diabetologia* 56, no. 3 (2013): 654–662, https://doi.org/10.1007/s00125-012-2789-5.

33. M. J. Romero, J. A. Iddings, D. H. Platt, et al., "Diabetes-Induced Vascular Dysfunction Involves Arginase I," *American Journal of Physiology—Heart and Circulatory Physiology* 302, no. 1 (2012): H159–H166, https://doi.org/10.1152/ajpheart.00774.2011.

34. Y. Tan, M. Ren, J. Hou, T. Hou, and X. Lin, "Increased CD14+HLA-DR-/low Myeloid-Derived Suppressor Cells Can Be Regarded as a Biomarker on Disease Severity and Response to Therapy in Acute Coronary Syndrome," *PeerJ* 12 (2024): e18154, https://doi.org/10.7717/peerj.18154.

35. Y. Lu, N. Zhao, and Y. Du, "Comprehensive Bioinformatics Analysis Reveals Common Potential Mechanisms, Progression Markers, and Immune Cells of Coronary Virus Disease 2019 and Atrial Fibrillation," *Frontiers in Cardiovascular Medicine* 9 (2022): 1027026, https://doi.org/10.3389/fcvm.2022.1027026.

36. B. Rastegari, A. G. Talepoor, S. Khosropanah, and M. Doroudchi, "In Vitro Targeted Delivery of Simvastatin and Niacin to Macrophages Using Mannan-Grafted Magnetite Nanoparticles," *ACS Omega* 9, no. 1 (2024): 658–674, https://doi.org/10.1021/acsomega.3c06389.

37. J. Dumont, M. Zureik, D. Cottel, et al., "Association of Arginase 1 Gene Polymorphisms With the Risk of Myocardial Infarction and Common Carotid Intima Media Thickness," *Journal of Medical Genetics* 44, no. 8 (2007): 526–531, https://doi.org/10.1136/jmg.2006.047449.

38. J. G. Schnitzler, R. M. Hoogeveen, L. Ali, et al., "Atherogenic Lipoprotein(A) Increases Vascular Glycolysis, Thereby Facilitating Inflammation and Leukocyte Extravasation," *Circulation Research* 126, no. 10 (2020): 1346–1359, https://doi.org/10.1161/CIRCRESAHA.119.316206.

39. A. T. H. Wu, L. Bashir, Y.-M. Tzeng, C.-C. Shih, and C.-M. Shih, "Identification of a Novel Theranostic Signature of Metabolic and Immune-Inflammatory Dysregulation in Myocardial Infarction, and the Potential Therapeutic Properties of Ovatodiolide, a Diterpenoid Derivative," *International Journal of Molecular Sciences* 23, no. 3 (2022): 1281, https://doi.org/10.3390/ijms23031281.

40. K. Poels, J. G. Schnitzler, F. Waissi, et al., "Inhibition of PFKFB3 Hampers the Progression of Atherosclerosis and Promotes Plaque Stability," *Frontiers in Cell and Developmental Biology* 8 (2020): 581641, https://doi.org/10.3389/fcell.2020.581641.

41. X. Zhang, B. Zheng, L. Zhao, et al., "KLF4-PFKFB3-Driven Glycolysis Is Essential for Phenotypic Switching of Vascular Smooth Muscle Cells," *Communications Biology* 5, no. 1 (2022): 1332, https://doi.org/10.1038/s42003-022-04302-y.

42. X. Wang, X. Liu, W. Wu, et al., "Hypoxia Activates Macrophage-NLRP3 Inflammasome Promoting Atherosclerosis via PFKFB3-Driven Glycolysis," *Federation of American Societies for Experimental Biology Journal: Official Publication of the Federation of American Societies For Experimental Biology* 38, no. 15 (2024): e23854, https://doi.org/10.1096/fj.202400283R.

43. S. Guo, A. Li, X. Fu, et al., "Gene-Dosage Effect of Pfkfb3 on Monocyte/Macrophage Biology in Atherosclerosis," *British Journal of Pharmacology* 179, no. 21 (2022): 4974–4991, https://doi.org/10.1111/bph.15926.

44. S. He, H. Zhu, J. Zhang, X. Yang, and Z. Lei, "Genome-Wide Screening for Circrnas in Epicardial Adipose Tissue of Heart Failure Patients With Preserved Ejection Fraction," *American Journal of Tourism Research* 15, no. 7 (2023): 4610–4619.

45. K.-S. Choi, H.-J. Choi, J.-K. Lee, et al., "The Endothelial E3 Ligase HECW2 Promotes Endothelial Cell Junctions by Increasing AMOTL1 Protein Stability via K63-linked Ubiquitination," *Cellular Signalling* 28, no. 11 (2016): 1642–1651, https://doi.org/10.1016/j.cellsig.2016.07.015.

46. J. Halvardson, J. J. Zhao, A. Zaghlool, et al., "Mutations in HECW2 Are Associated With Intellectual Disability and Epilepsy," *Journal of Medical Genetics* 53, no. 10 (2016): 697–704, https://doi.org/10.1136/jmedgenet-2016-103814.

47. E. R. Berko, M. T. Cho, C. Eng, et al., "De Novo Missense Variants in HECW2 Are Associated With Neurodevelopmental Delay and Hypotonia," *Journal of Medical Genetics* 54, no. 2 (2017): 84–86, https://doi.org/10.1136/jmedgenet-2016-103943.

48. J. Lian, C. Zhang, and H. Lu, "A Ferroptosis-Related Lncrna Signature Associated With Prognosis, Tumor Immune Environment, and Genome Instability in Hepatocellular Carcinoma," *Computational and Mathematical Methods in Medicine* 2022 (2022): 6284540, https://doi.org/10.1155/2022/6284540.

49. Y. Li, S. Liu, L. Wen, et al., "Profiling Immune Cell-Related Gene Features and Immunoregulatory Cerna in Ischemic Stroke," *Molecular Biomedicine* 5, no. 1 (2024): 72, https://doi.org/10.1186/s43556-024-00237-4.

50. X. Yang, K. K. Mann, H. Wu, and J. Ding, "Sccross: A Deep Generative Model for Unifying Single-Cell Multi-Omics With Seamless Integration, Cross-Modal Generation, and in Silico Exploration,"

Genome Biology 25, no. 1 (2024): 198, https://doi.org/10.1186/s13059-024-03338-z.

51. P. Zhang, H. Zhang, and H. Wu, "iPro-WAEL: A Comprehensive and Robust Framework for Identifying Promoters in Multiple Species," *Nucleic Acids Research* 50, no. 18 (2022): 10278–10289, https://doi.org/10.1093/nar/gkac824.

52. X. Zhou and H. Wu, "Schiclassifier: A Deep Learning Framework for Cell Type Prediction by Fusing Multiple Feature Sets From Single-Cell Hi-C Data," *Briefings in Bioinformatics* 26, no. 1 (2024): bbaf009, https://doi.org/10.1093/bib/bbaf009.

53. Y. Wu, Y. Xu, and L. Xu, "Pharmacological Therapy Targeting the Immune Response in Atherosclerosis," *International Immunopharmacology* 141 (2024): 112974, https://doi.org/10.1016/j.intimp.2024.112974.

54. M. Zhangyu, B. Xiao, Li Dianguo, X. Wen, Y. Fan, and H. Wu, "DHHNN: A Dynamic Hypergraph Hyperbolic Neural Network Based on Variational Autoencoder for Multimodal Data Integration and Node Classification," *Information Fusion* 119 (2025): 103016, https://doi.org/10.1016/j.inffus.2025.103016.

Supporting Information

Additional supporting information can be found online in the Supporting Information section.
Supporting Information S1: syb270039-sup-0001-suppl-data.docx. **Supporting Information S2:** syb270039-sup-0002-suppl-data.docx. **Table S1:** Differential Analysis Results. **Table S2:** Enrichment Analysis of Differentially Expressed Genes.